

Non-linear effects in Solar Wind and Magnetosphere plasmas: PIC simulations and theory

Electromagnetic electron hole generation



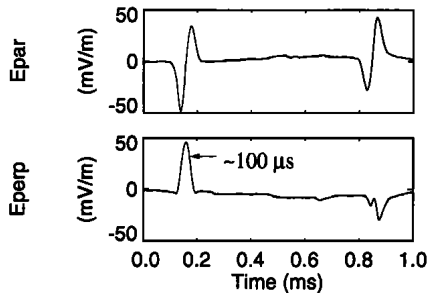
G. Gauthier, T. Chust, O. Le Contel, P. Savoini

Elbereth conference – February 9, 2021

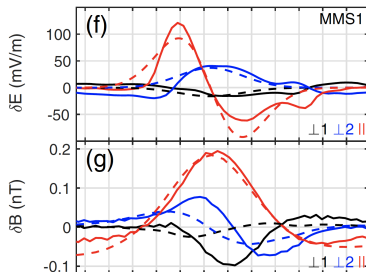


Satellites exploring the magnetospheric plasma have several times reported the *observation of solitary potential structures* [Vasko 2017, Le Contel 2017, Holmes 2018, Steinvall 2019].

Electrostatic obs [Ergun 1998]

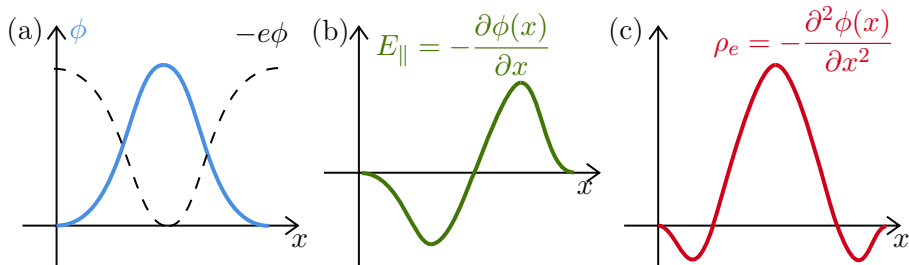


Electromagnetic obs [Steinvall 2019]



Solitary waves are observed in **various regions of the Earth's magnetosphere.**

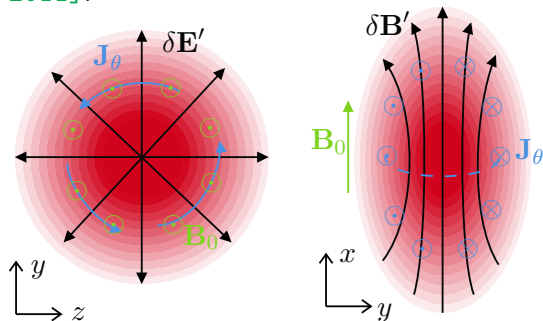
Electron phase-space holes (EH) are a *kinetic-scale plasma structures* ($\sim 10\lambda_D$) and persist during long time ($\tau \gg 10\omega_p^{-1}$).



EH = spatial structures measured by temporal spacecraft setup

They are characterized by a *bipolar electric field* $E_{||}$ parallel to the magnetic field $\mathbf{B}_0 = B_0 \mathbf{e}_x$ with a positive electric potential $\phi(x)$, caused by a self-consistent *decrease in density of electrons* $n_e(x) = -\rho_e/e$ in interaction with this potential.

Qualitative illustration of *electromagnetic EH model* [adapted from Tao 2011]:



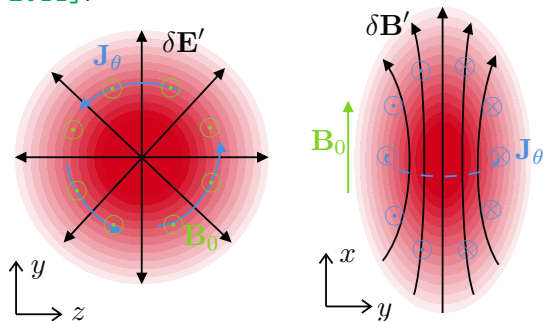
The **total EH magnetic field** including this effect is found using a *Lorentz transformation* ($\gamma \sim 1$):

$$\delta \mathbf{B} = \delta \mathbf{B}' - \frac{1}{c^2} \mathbf{v}_{\text{EH}} \times \mathbf{E}$$

where $\delta \mathbf{B}'$ is obtained by *Biot and Savart*:

$$\delta \mathbf{B}' = \frac{\mu_0}{4\pi} \iiint \mathbf{J}_\theta(\boldsymbol{\xi}) \frac{\mathbf{x} - \boldsymbol{\xi}}{|\mathbf{x} - \boldsymbol{\xi}|^3} d^3 \boldsymbol{\xi}$$

Qualitative illustration of *electromagnetic EH model* [adapted from Tao 2011]:



The **total EH magnetic field** including this effect is found using a *Lorentz transformation* ($\gamma \sim 1$):

$$\delta \mathbf{B} = \delta \mathbf{B}' - \frac{1}{c^2} \mathbf{v}_{\text{EH}} \times \mathbf{E}$$

where $\delta \mathbf{B}'$ is obtained by *Biot and Savart*:

$$\delta \mathbf{B}' = \frac{\mu_0}{4\pi} \iiint \mathbf{J}_\theta(\boldsymbol{\xi}) \frac{\mathbf{x} - \boldsymbol{\xi}}{|\mathbf{x} - \boldsymbol{\xi}|^3} d^3 \boldsymbol{\xi}$$

Questions :

1. What are the possible sources of generation?
2. What are 3D EH properties in ambient magnetic field?

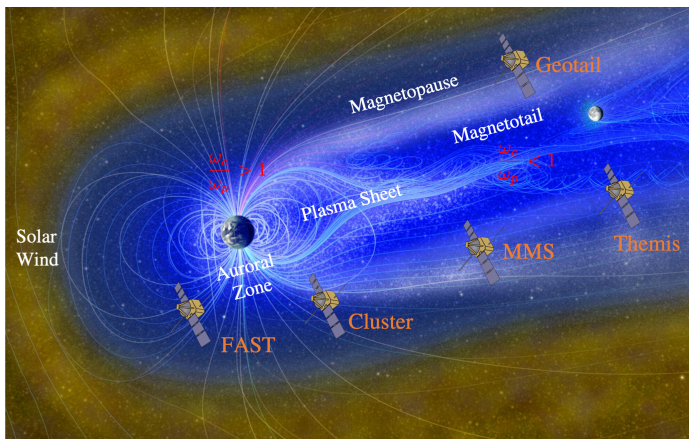
Spacecraft missions (Geotail, FAST, Cluster, THEMIS, MMS ...) have measured two types of moving structures:

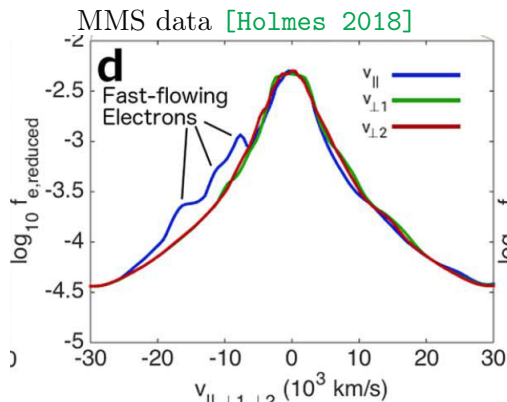
- *Fast structures* ($v \sim c/4$),
- *Slow structures* ($v \leq c/10$).

Electron holes (EHs) typically form from *thermalizing mechanisms*:

- **unstable counterstreaming instability**,
- **bump-on-tail instability**,
resulting of between *two different plasma populations* or *accelerated beam driven* (e.g. plasma double layer, magnetic reconnection, astrophysical jets).

⇒ *It is possible to simulate this with a PIC code.*





Using SMILEI PIC code with *magnetospheric plasma physical parameters*:

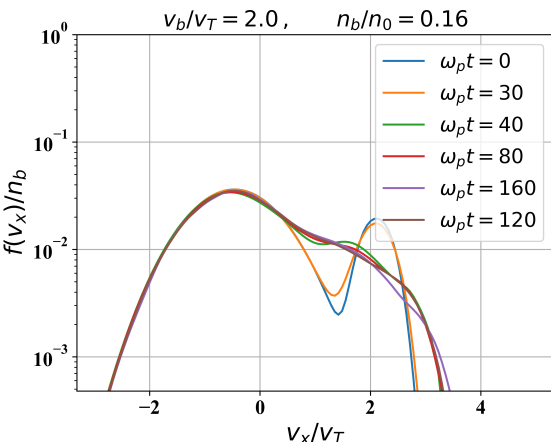
$$T_e = 16 T_b = 4 \text{ keV}, \quad T_i = [1 - 10] T_e,$$

$$v_b = [2 - 4] v_T, \quad n_b = [0.05 - 0.2] n_0,$$

$$\omega_c = [0.8 - 5.0] \omega_p, \quad \mathbf{B} = B_0 \mathbf{e}_x,$$

$$\mu = m/M = 1/1836$$

Solitary waves in the magnetotail are three-dimensional potentials generated through *nonlinear evolution* of an **electron bump-on-tail instability**.



Using SMILEI PIC code with *magnetospheric plasma physical parameters*:

$$T_e = 16 T_b = 4 \text{ keV}, \quad T_i = [1 - 10] T_e,$$

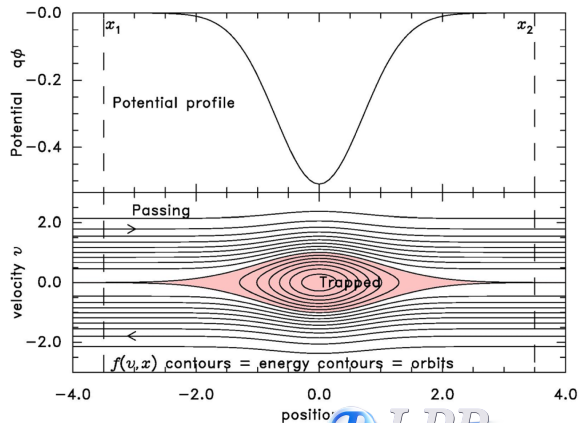
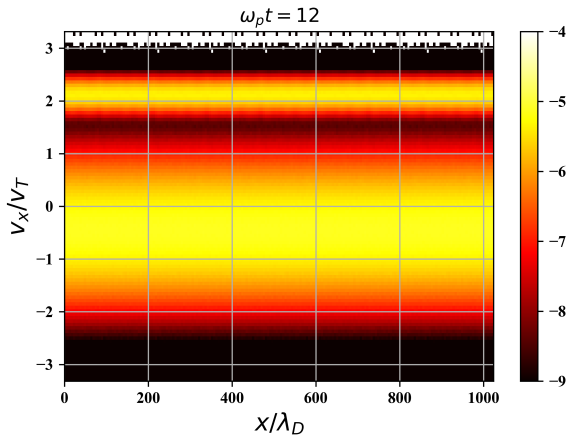
$$v_b = [2 - 4] v_T, \quad n_b = [0.05 - 0.2] n_0,$$

$$\omega_c = [0.8 - 5.0] \omega_p, \quad \mathbf{B} = B_0 \mathbf{e}_x,$$

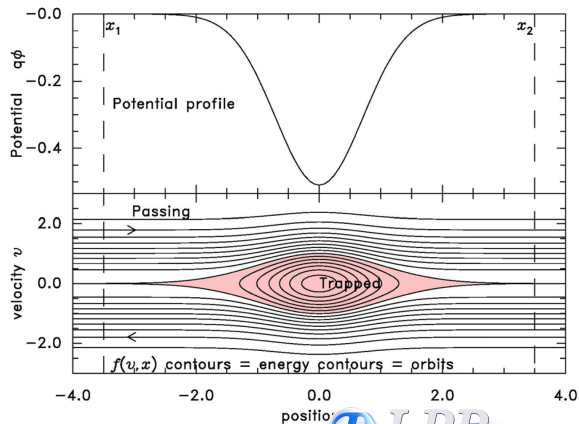
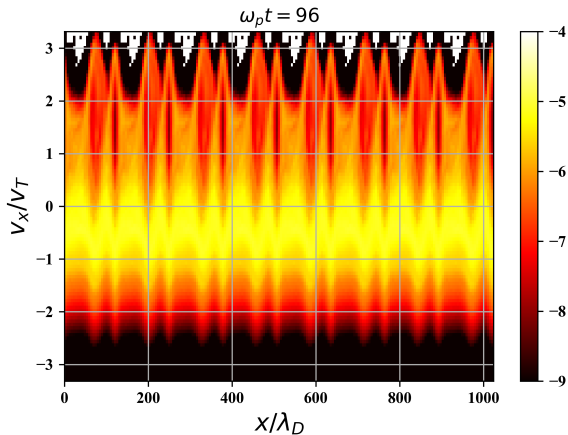
$$\mu = m/M = 1/1836$$

Solitary waves in the magnetotail are three-dimensional potentials generated through *nonlinear evolution* of an **electron bump-on-tail instability**.

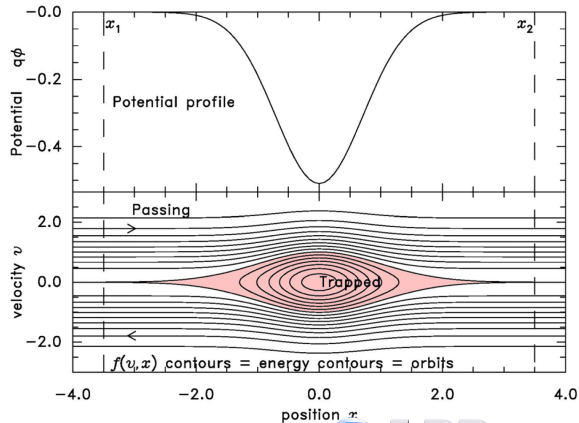
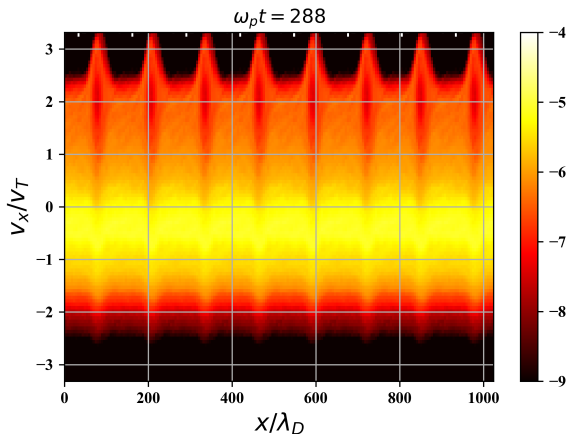
EH are generated with **PIC simulations** \Rightarrow *cylindrical three-dimensional potentials* which can be generated through nonlinear evolution of an electron beam instability

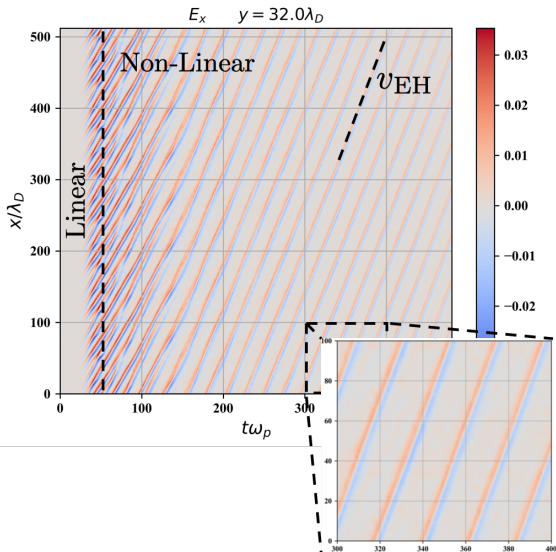


EH are generated with **PIC simulations** \Rightarrow *cylindrical three-dimensional potentials* which can be generated through nonlinear evolution of an electron beam instability



EH are generated with **PIC simulations** \Rightarrow *cylindrical three-dimensional potentials* which can be generated through nonlinear evolution of an electron beam instability





Form Lorentz eq:

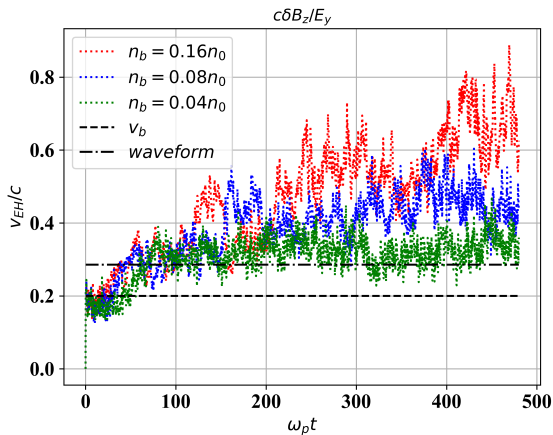
$$\delta \mathbf{B}' - \delta \mathbf{B} = \frac{1}{c^2} \mathbf{v}_{EH} \times \mathbf{E}$$

Common assumption [Anderson 2009] :

- Perpendicular magnetic field,
- $\mathbf{v}_{EH} = v_{EH} \mathbf{e}_{\parallel}$,
- $\delta \mathbf{B}' = \mathbf{0}$ ($\delta \mathbf{E} \times \mathbf{B}_0$ drift ignored),

allows to calculate:

$$v_{EH} = c^2 \frac{\delta B_{\perp}}{\delta E_{\parallel}}$$



Form Lorentz eq:

$$\delta \mathbf{B}' - \delta \mathbf{B} = \frac{1}{c^2} \mathbf{v}_{\text{EH}} \times \mathbf{E}$$

Common assumption [Anderson 2009] :

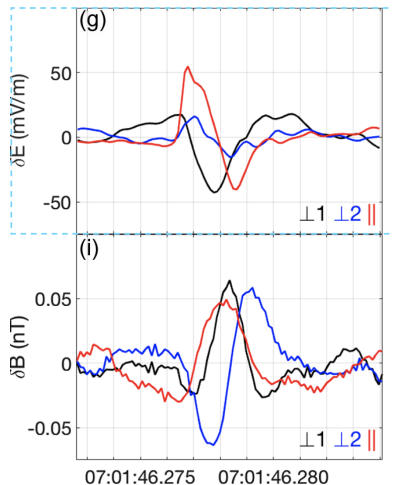
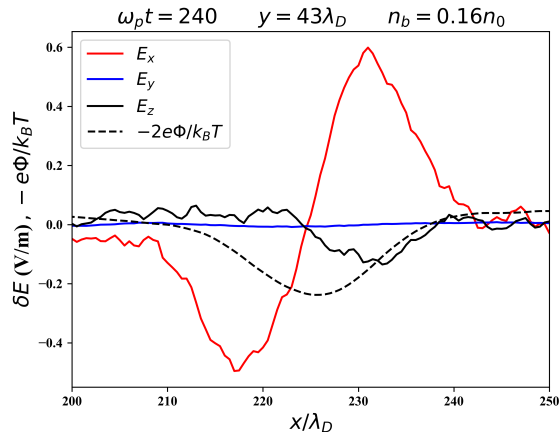
- Perpendicular magnetic field,
- $\mathbf{v}_{\text{EH}} = v_{\text{EH}} \mathbf{e}_{\parallel}$,
- $\delta \mathbf{B}' = \mathbf{0}$ ($\delta \mathbf{E} \times \mathbf{B}_0$ drift ignored),

allows to calculate:

$$v_{\text{EH}} = c^2 \frac{\delta B_{\perp}}{\delta E_{\parallel}}$$

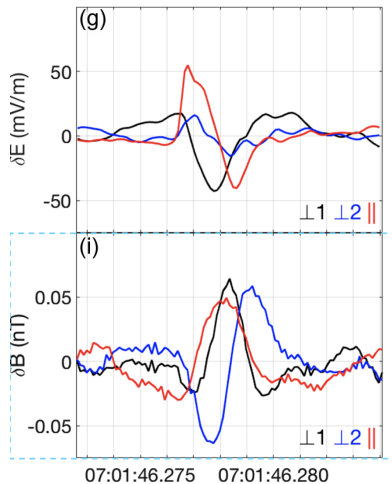
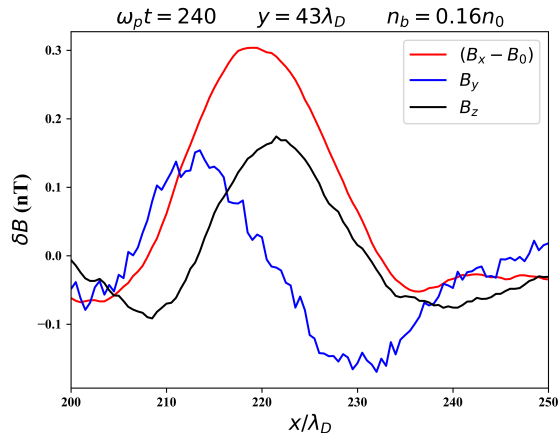
\Rightarrow we *cannot neglect induce* $\delta \mathbf{B}' \propto \mathbf{J}_{\theta}(n_b)$

Examples of EH *induced fields shapes*



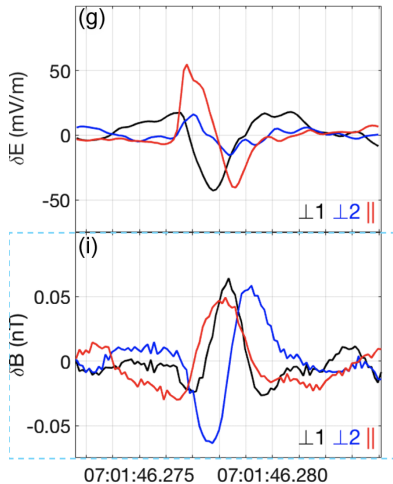
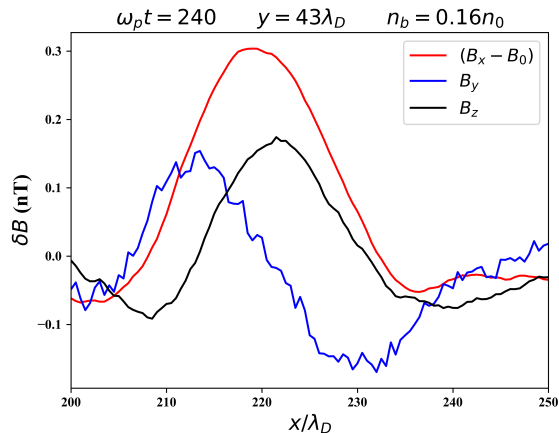
[Steinvall 2019]

Examples of EH *induced fields shapes*



[Steinvall 2019]

Examples of EH *induced fields shapes*



[Steinvall 2019]

\Rightarrow **PIC simulations can generate quantitatively and qualitatively EH**

EH exists in different regions of magnetosphere \Rightarrow We need to taking account of **ambient magnetic field value** $\|\mathbf{B}_0\|$ ($\equiv \omega_c/\omega_p$).

Due to $\varrho_{Li} \gg \varrho_{Le}$ and $\omega_p \sim \omega_c \gg \omega_b$: bounce frequency \Rightarrow add *electronic polarisation effects* (ions are frozen) as a perpendicular perturbation:

$$\mathbf{J}_{\text{pol}} = \varepsilon_0 \frac{\omega_p^2}{\omega_c^2} \frac{\partial(\nabla_{\perp} \phi)}{\partial t} \quad \Rightarrow \quad \nabla \cdot \mathbf{J}_{\text{pol}} = -\frac{\partial}{\partial t} \left[\nabla \cdot \left(\frac{\omega_p^2}{\omega_c^2} \nabla_{\perp} \phi \right) \right] = -\frac{\partial \rho_{\text{pol}}}{\partial t}$$

Hence we modify **Vlasov-Poisson system** [Lee 1983, Vasko 2017] in cylindrical coordinates (r, θ, x) along magnetic field as:

$$\mathbf{v} \cdot \nabla f_s(\mathbf{x}, \mathbf{v}) - \left[\frac{q_s}{m_s} \nabla \phi - \omega_{cs}(\mathbf{v} \times \mathbf{e}_x) \right] \cdot \frac{\partial f_s(\mathbf{x}, \mathbf{v})}{\partial \mathbf{v}} = 0$$

$$\nabla^2 \phi(\mathbf{x}) = -\frac{(\rho(\mathbf{x}) + \rho_{\text{pol}})}{\varepsilon_0}$$

EH exists in different regions of magnetosphere \Rightarrow We need to taking account of **ambient magnetic field value** $\|\mathbf{B}_0\|$ ($\equiv \omega_c/\omega_p$).

Due to $\varrho_{Li} \gg \varrho_{Le}$ and $\omega_p \sim \omega_c \gg \omega_b$: bounce frequency \Rightarrow add *electronic polarisation effects* (ions are frozen) as a perpendicular perturbation:

$$\mathbf{J}_{\text{pol}} = \varepsilon_0 \frac{\omega_p^2}{\omega_c^2} \frac{\partial(\nabla_{\perp} \phi)}{\partial t} \quad \Rightarrow \quad \nabla \cdot \mathbf{J}_{\text{pol}} = -\frac{\partial}{\partial t} \left[\nabla \cdot \left(\frac{\omega_p^2}{\omega_c^2} \nabla_{\perp} \phi \right) \right] = -\frac{\partial \rho_{\text{pol}}}{\partial t}$$

Hence we modify **Vlasov-Poisson system** [Lee 1983, Vasko 2017] in cylindrical coordinates (r, θ, x) along magnetic field as:

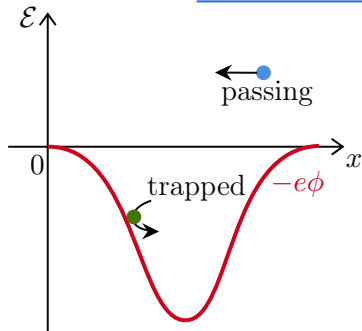
$$\mathbf{v} \cdot \nabla f_s(\mathbf{x}, \mathbf{v}) - \left[\frac{q_s}{m_s} \nabla \phi - \omega_{cs} (\mathbf{v} \times \mathbf{e}_x) \right] \cdot \frac{\partial f_s(\mathbf{x}, \mathbf{v})}{\partial \mathbf{v}} = 0$$

$$\frac{\partial^2 \phi(\mathbf{x})}{\partial x^2} + \underbrace{\left(1 + \frac{\omega_p^2}{\omega_c^2} \right)}_{=\Omega} \nabla_{\perp}^2 \phi(\mathbf{x}) = -\frac{\rho(\mathbf{x})}{\varepsilon_0}$$

Introducing $\mathcal{E} = m_s v^2/2 + q_s \phi(x) = C^{\text{st}}$ along a magnetic line, electron distribution function could be separated in two families:

$$f_e(\mathcal{E}) = \begin{cases} f_p(\mathcal{E}), & \mathcal{E} \geq 0 \\ f_t(\mathcal{E}), & \mathcal{E} < 0 \end{cases}$$

with "at ∞ " condition : $f_p(\mathcal{E} \rightarrow \infty) = f_e(\mathcal{E})$. Hence,
Poisson equation become:



$$\int_{-e\phi}^0 \frac{f_t(\mathcal{E}) d\mathcal{E}}{\sqrt{2m(\mathcal{E} + e\phi)}} = \frac{\varepsilon_0}{e} \frac{\partial^2 \phi(\mathbf{x})}{\partial x^2} + \frac{\varepsilon_0 \Omega}{e} \nabla_{\perp}^2 \phi(\mathbf{x}) - \int_0^{+\infty} \frac{f_p(\mathcal{E}) d\mathcal{E}}{\sqrt{2m(\mathcal{E} + e\phi)}} + \int_{e\phi}^{+\infty} \frac{f_i(\mathcal{E}) d\mathcal{E}}{\sqrt{2M(\mathcal{E} - e\phi)}} = \mathbf{g}(e\phi)$$

$f_t(\mathcal{E})$ is defined over the half-space $\mathcal{E} < 0$, we obtain (where $\mathbf{g}(0) = 0$):

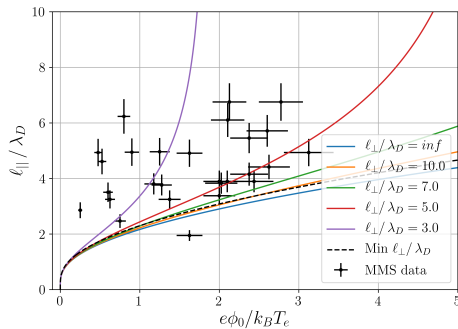
$$f_t(\mathcal{E}) = \frac{\sqrt{2m}}{\pi} \int_0^{-\mathcal{E}} \frac{d\mathbf{g}(\mathcal{V})}{d\mathcal{V}} \frac{d\mathcal{V}}{\sqrt{-\mathcal{E} - \mathcal{V}}} = \mathcal{I}_{\phi}(\phi_{\parallel}) + \mathcal{I}_B(\phi_{\perp}, \Omega) + \mathcal{I}_{\text{passing}}(f_p) + \mathcal{I}_{\text{ions}} \ll 1$$

From MMS observations (*e.g.* [Holmes 2018]), we assume:

$$\phi(r, x) = \phi_0 \exp(-x^2/2\ell_{\parallel}^2) \exp(-r^2/2\ell_{\perp}^2)$$

and $f_p(\mathcal{E})$ as a Maxwellian. The **trapped electron distribution function** *must be physical* $f_t(\mathcal{E} = -e\phi_0) \geq 0$, we obtain *two existence criterion* (where $\Omega^2 = 1 + \omega_p^2/\omega_c^2$):

$$\begin{cases} \frac{\ell_{\parallel}}{\lambda_D} \geq \sqrt{\frac{(4 \ln 2 - 1)}{\sqrt{\pi} e^{\beta e \phi_0} [1 - \operatorname{erf}(\sqrt{\beta e \phi_0})]/2\sqrt{\beta e \phi_0} - \Omega^2 \lambda_D^2 / \ell_{\perp}^2}} \\ \frac{\ell_{\perp}}{\lambda_D} \geq \frac{\Omega}{\sqrt{\sqrt{\pi} e^{\beta e \phi_0} [1 - \operatorname{erf}(\sqrt{\beta e \phi_0})]/2\sqrt{\beta e \phi_0}}} \end{cases} \Rightarrow \frac{\ell_{\parallel}}{\ell_{\perp}} \simeq \sqrt{\Omega}$$



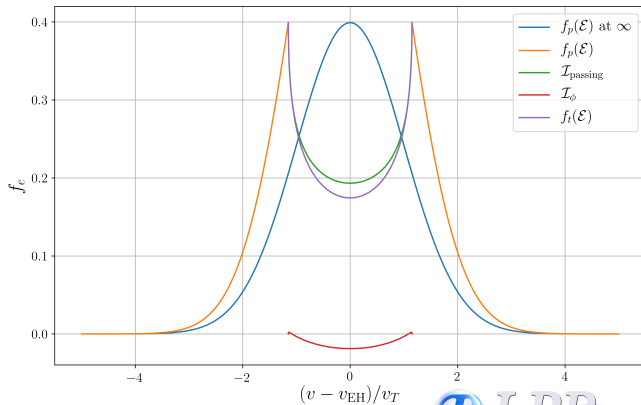
\Rightarrow *3D shape of potential* ($\parallel + \perp$) and *magnetic value* $\|\mathbf{B}_0\|$ impact on EH existence

$f_t(\mathcal{E})$ calculation depends on the choice of the potential $\phi(x)$ and $f_p(\mathcal{E})$:

$$f_p(\mathcal{E}) \text{ "at } \infty" = \frac{n_0}{\sqrt{2\pi}v_T} \sum_{\sigma=\pm 1} \exp \left[-\frac{(\sigma\sqrt{2\mathcal{E}/m} - u_e)^2}{2v_T^2} \right]$$

$u_e = 0$ case:

- *Analytic solution* for $\mathcal{I}_{\text{passing}}$,
- $f_t(\mathcal{E}) = \mathcal{I}_{\phi} + \mathcal{I}_{\text{passing}}$,
- $v_b = v_{\text{EH}}$ cannot represent a realistic model.

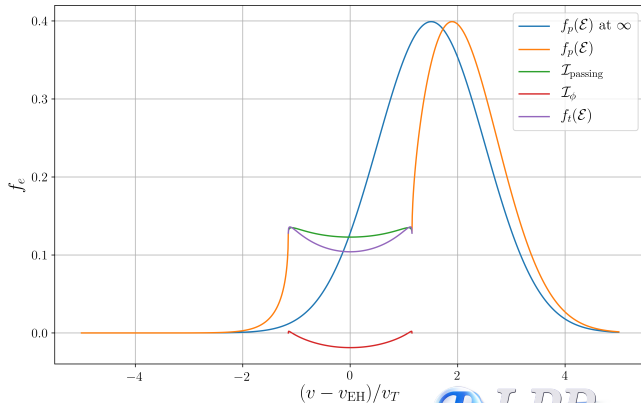


$f_t(\mathcal{E})$ calculation depends on the choice of the potential $\phi(x)$ and $f_p(\mathcal{E})$:

$$f_p(\mathcal{E}) \text{ "at } \infty" = \frac{n_0}{\sqrt{2\pi}v_T} \sum_{\sigma=\pm 1} \exp \left[-\frac{(\sigma\sqrt{2\mathcal{E}/m} - u_e)^2}{2v_T^2} \right]$$

$u_e \neq 0$ case:

- *Numerical solution* for $\mathcal{I}_{\text{passing}}$,
- $f_t(\mathcal{E}) = \mathcal{I}_{\phi} + \mathcal{I}_{\text{passing}}$,
- $v_b \neq v_{\text{EH}}$ can represent a realistic model.



Conclusion

- We showed that we are able to generate EH by **PIC code** using *bump-on-tail instability* with *real magnetospheric plasma physical parameters*,
- Simulated EH are **comparable** to EH MMS measurements,
- **BGK model** could be adjust in *3D* and with *magnetospheric ambient magnetic field* $\|\mathbf{B}_0\|$.